

UNCLASSIFIED

Defense Technical Information Center  
Compilation Part Notice

ADP012222

TITLE: Controlling the Microstructure and Magnetic Properties of  
Ferromagnetic Nanocrystals Produced by Ion Implantation

DISTRIBUTION: Approved for public release, distribution unlimited

This paper is part of the following report:

TITLE: Nanophase and Nanocomposite Materials IV held in Boston,  
Massachusetts on November 26-29, 2001

To order the complete compilation report, use: ADA401575

The component part is provided here to allow users access to individually authored sections of proceedings, annals, symposia, etc. However, the component should be considered within the context of the overall compilation report and not as a stand-alone technical report.

The following component part numbers comprise the compilation report:

ADP012174 thru ADP012259

UNCLASSIFIED

## Controlling the Microstructure and Magnetic Properties of Ferromagnetic Nanocrystals Produced by Ion Implantation.

K.S. Beaty,<sup>1</sup> A. Meldrum,<sup>1</sup> J.P. Franck,<sup>1</sup> K. Sorge,<sup>2</sup> J. R. Thompson,<sup>2</sup> C.W. White,<sup>3</sup> R.A. Zuhr,<sup>3</sup> L.A. Boatner,<sup>3</sup> S. Honda<sup>3</sup>

<sup>1</sup> The University of Alberta, Edmonton, AB

<sup>2</sup> The University of Tennessee, Knoxville, TN

<sup>3</sup> Oak Ridge National Laboratory, Oak Ridge, TN

### ABSTRACT

Ion implantation coupled with annealing is a versatile and flexible approach to creating ferromagnetic near-surface nanocomposites that represent a wide range of particle/host combinations. We have used ion implantation and thermal processing to create a layer of Co nanoparticles in a sapphire host that was subsequently irradiated with Xe, Pt, or Pb in order to systematically modify the magnetic properties of the composite. Transmission electron microscopy (reported in an accompanying paper in this volume) was used to carry out a detailed characterization of the microstructure of the resulting near-surface composites whose magnetic properties were determined using SQUID magnetometry or magnetic circular dichroism. These composites exhibit magnetic hysteresis with coercivities ranging from near zero (i.e., superparamagnetism) up to 1.2 kG – depending on the composition and microstructure. We also present the results of preliminary experiments in which we attempt to control the spatial distribution of magnetic elements within ion-implanted ferromagnetic nanocomposites. The results demonstrate methods for tailoring the magnetic properties of nanocomposites produced by ion implantation for specific applications.

### INTRODUCTION

Ion implantation was first used to create embedded magnetic nanoclusters over a decade ago [e.g., see Ref. 1]. By injecting varying concentrations of Fe, Co, or Ni into dielectric hosts such as crystalline  $\text{Al}_2\text{O}_3$  and fused  $\text{SiO}_2$ , relatively soft magnetic composites were created with low coercivities and a magnetic moment per atom similar to that of bulk magnetic material. Room-temperature superparamagnetism is often reported, due to particle sizes well below that needed to prevent random thermal reorientation of the particle magnetization. Blocking temperatures have been calculated from the precipitate sizes and anisotropy constants, and seem to agree reasonably well with experimentally observed blocking temperatures obtained from field-cooled and zero-field-cooled measurements of the magnetization. Nevertheless, a range of particle sizes is often reported, and the thermal blocking temperature is accordingly distributed over a range of temperatures. Furthermore, the effects of the dielectric host material on the magnetic properties of the composite are only rarely investigated or reported.

In previous ion implantation work, single-element nanoparticles (and in some cases, oxide particles) of Fe, Ni, or Co have been produced in either  $\text{SiO}_2$  glass or crystalline sapphire wafers [1]. More recently, additional motivation for research in this area has been provided by the potential for creating new materials with possible applications as magnetic recording media. Single-nanocrystal-per-bit data recording would represent an important advance in the information storage capacity of such media [2]. Nevertheless, several quite stringent

requirements must be met in order to achieve device-quality performance. For single-particle bits to be written individually, the precipitates must be discrete, magnetically isolated, ferromagnetic nanoparticles that are larger than the superparamagnetic limit and whose coercivity, size, orientation, and position can be controlled. Ferromagnetic nanoclusters produced by ion implantation can be formed as single domain particles that are larger than the superparamagnetic limit. The crystallographic orientation (and therefore, the magnetic anisotropy directions) can also be controlled by using single-crystal hosts [3,4]. However, the question of magnetic isolation is still problematic [5], size distributions are relatively wide, and there has been no effective in-plane control over the spatial distribution of the magnetic nanoclusters.

Here, we describe recent progress in exercising additional control over the magnetic properties of ferromagnetic nanocluster composites, and we discuss our initial attempts to control the in-plane spatial distribution of the magnetic nanoclusters. The present investigations focus on the magnetic characteristics of Co nanoclusters formed by ion implantation and annealing of a single-crystal sapphire wafer, and we explore the magnetic properties of  $\text{Al}_2\text{O}_3$ -Co nanocomposites irradiated with either Xe, Pt, or Pb ions. Ion irradiation of pre-existing nanoclusters dramatically modifies the magnetic characteristics [3] and establishes a means for tailoring the materials properties. Finally, we report on the initial results of micron- and sub-micron-scale ion-beam patterning using ion implantation.

## EXPERIMENTAL

In the ion implantation technique, high-energy ions are injected into a selected host material, producing a supersaturation of implanted material in the near-surface region. During a subsequent thermal processing step, the implanted material nucleates as discrete nanoscale precipitates embedded below the surface of the host. In our experiments, high-purity single-crystal sapphire wafers were implanted at room temperature with 140 keV  $\text{Co}^+$  to an ion fluence of  $8 \times 10^{16}$  ions/cm<sup>2</sup>. In order to induce precipitate formation, the specimens were subsequently annealed in a quartz tube furnace for 2 hours at 1100 °C under Ar+4%  $\text{H}_2$  atmosphere. The specimens were retracted out of the hot-zone in order to cool rapidly to room temperature. X-ray and electron diffraction measurements were used to determine the structure and orientation of the resulting precipitates. In order to investigate the effects of ion irradiation on the Co nanoparticles, the specimens were subsequently irradiated with either 244 keV Xe or 320 keV Pt ions. These ions were chosen to create maximum displacement damage in the Co-nanoparticle layer, while either minimizing (Xe) or intentionally inducing (Pt) chemical effects due to the implanted impurities. Ion energies were selected to give a similar projected range for both species. Magnetic measurements were done using a SQUID magnetometer or by magnetic circular dichroism.

## RESULTS AND DISCUSSION

### Control over the magnetic properties

Figure 1 shows a cross-sectional image of a sapphire wafer implanted with  $8 \times 10^{16}$  ions/cm<sup>2</sup>  $\text{Co}^+$  at room

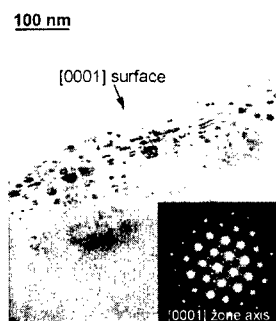


Fig. 1. Cross sectional TEM image of the Co nanocrystals in  $\text{Al}_2\text{O}_3$ . An electron diffraction pattern is shown in the inset.

temperature and subsequently annealed for two hours at 1100°C followed by a rapid cool-down. The resulting nanocrystals extend to a depth of ~120 nm in the host sapphire. The nanoparticles are either rounded or faceted, depending on their depth below the surface. This depth dependence of the precipitate morphology is discussed in more detail in a TEM investigation in an accompanying paper in this volume [6]. The precipitates are crystallographically aligned with the sapphire, as demonstrated by the double-diffraction spots in the electron diffraction pattern in Fig. 1. X-ray diffraction results (not shown here) showed that both the hexagonal and cubic phases of cobalt are present in roughly equal amounts.

Magnetic hysteresis measurements for this specimen are shown in Figure 2. These data, obtained by SQUID magnetometry, were corrected to eliminate the effect of the diamagnetic sapphire host. The coercivity of the Co nanoparticles for an applied field perpendicular to the specimen surface is approximately 150 G and the saturation moment is  $\sim 2.3 \times 10^4$  G/cm<sup>3</sup>. These values are slightly lower when the field is applied parallel to the specimen surface. After implantation with 320 keV Pt to a fluence of  $6.4 \times 10^{15}$  ions/cm<sup>2</sup>, the field-perpendicular hysteresis loop broadened considerably (Fig. 3). The saturation magnetization decreased to  $\sim 2.0 \times 10^4$  G/cm<sup>3</sup>, but the coercivity increased from 150 G to 1.14 kG. A TEM investigation of this specimen [6], shows that Pt irradiation amorphizes the host sapphire, but that the Co precipitates remain crystalline and do not lose their original crystallographic alignment.

In Figure 4, we compare the effects of 244 keV Xe and 320 keV Pt irradiation on the field-perpendicular coercivity of the Co nanoclusters for varying ion doses. For the Xe irradiation, the coercivity of the Co-sapphire nanocomposite increases rapidly at first, but then levels off at ~500 G. For the Pt-irradiated sample, the coercivity saturates at ~1.2 kG.

There are several possible reasons for the magnetic hardening observed with increasing radiation dose. First, defects and defect clusters may pin the magnetization of the particles, as has been observed in magnetic thin film materials [e.g., Ref. 7]. This pinning effect could inhibit the reorientation of the magnetization, thereby increasing the coercive field. Radiation-damage investigations show damage saturation at some level that

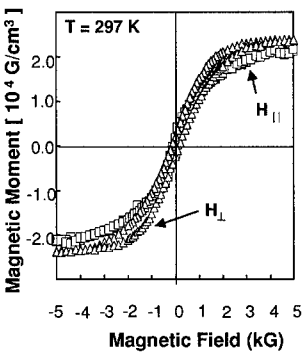


Fig. 2. Magnetic hysteresis measurements for magnetic field parallel or perpendicular to the plane of Co precipitates.

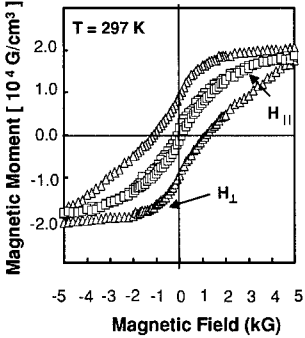


Fig. 3. Same as Fig. 2, after a subsequent implantation Pt to a fluence of  $6.4 \times 10^{15}$  ions/cm<sup>2</sup>.

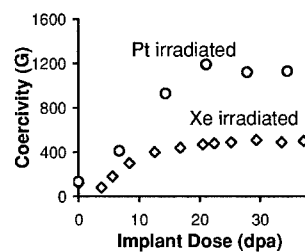


Fig. 4. MCD measurements of the coercive field as a function of dose for the Al<sub>2</sub>O<sub>3</sub>-Co specimen implanted with Xe or Pt.

depends on the kinetics of defect production and recombination [e.g., Ref. 8]. This saturation may be reflected in the “leveling off” of the coercive field at high ion doses. An additional factor may be due to the amorphization of the host sapphire. Sapphire undergoes a volume expansion during the crystalline-amorphous transition, which may place the precipitates under a directional stress. We have found that specimens irradiated at 100 °C to high doses with Pb, as opposed to the RT implants done here, show little increase in the coercivity and the  $\text{Al}_2\text{O}_3$  is not amorphized. The atomic-scale processes responsible for the large increase in the coercivity of the Pt-irradiated specimens, as compared to the Xe-irradiated case, is still under investigation. If the injected Pt reacts with the Co, atomic-scale domains of a CoPt alloy - a magnetic material with high coercivity - may exist within the nanocrystals.

These results suggest means by which the magnetic properties of ferromagnetic nanocomposites produced by ion implantation can be precisely controlled, and hard magnetic materials with high coercivities can be readily obtained. It is possible to create a Co-nanocluster composite whose magnetic coercivity, for example, can be tailored between 150 and 1,120 G. We also have found that even higher coercivities can be obtained by annealing to form CoPt alloy particles.

### Fine spatial control of the magnetic properties

One of the outstanding drawbacks of the ion implantation technique is the lack of adequate spatial control over the nanoparticle location. Focused ion beams have some promise for patterning with “manufacturer-claimed” beam diameters of < 10 nm at the specimen surface. Focused ion beam devices currently available, however, have been developed mainly as cutting or thinning tools and are very limited in both source type (mainly Ga) and energy range (< 35 kV). At this low energy, sputtering processes dominate [1]. An alternate method that is currently being explored is the patterning of implanted materials through lithographic masking. This is a method that has been extensively used in the microelectronics industry for spatial selection of regions to be doped using ion implantation [9], and it has recently been applied to the patterning of the magnetic properties of Co/Pt magnetic multilayers through ion irradiation [10].

For these initial investigations, fused  $\text{SiO}_2$  was selected as the host and Fe as the implant material. Fe was selected because the microstructural properties of implanted Fe have been well studied [e.g., 4,11,12]. Additionally, our work on Co precipitates shows that the nanoparticles have different crystal structures, complicating the interpretation of the magnetic results. The first step in the masking/implanting procedure is to create a patterned mask on top of the host material ( $\text{SiO}_2$ ). The masking material must have a high stopping power, adhere well to the substrate, be easily removed from the substrate after implantation, and have low sputtering yield. It must also withstand high-dose ion implantation without significant physical degradation. Based on these requirements, we grew sputter-deposited films of Cr and Mo directly on the  $\text{SiO}_2$  wafers (Fig. 5). In general, the Cr films oxidized quickly and gave less consistent lithographic patterns. Standard deep UV lithography was used to transfer the pattern from a specially designed mask with features ranging from 10.0 to 0.5 microns, followed by wet chemical etching and removal of photoresist.

The masked substrates were then implanted with 80 keV  $\text{Fe}^+$  to fluences of either  $1.5 \times 10^{17}$  ions/cm<sup>2</sup> or  $5 \times 10^{16}$  ions/cm<sup>2</sup>. Scanning electron microscopy (SEM) images of a representative mask before and after implantation are shown in Figs. 6 and 7. The implantation

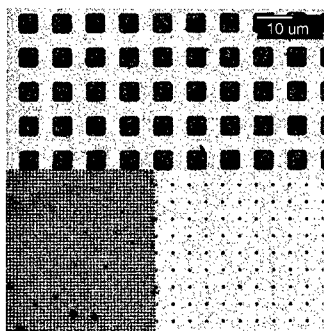


Fig. 5. Mo mask on SiO<sub>2</sub>. The hole sizes range from almost 10 μm to less than 1 μm across.

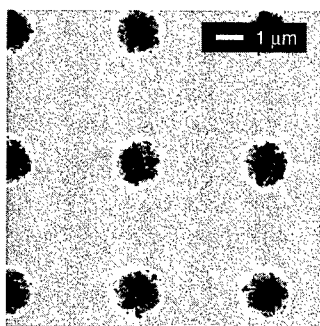


Fig. 6. A 380-nm-thick Mo mask on SiO<sub>2</sub>. The hole-bottoms contain residual material.

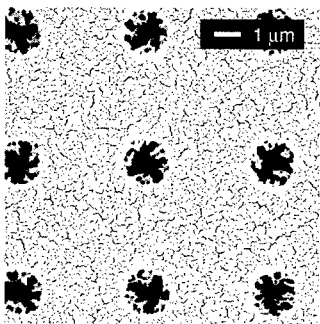


Fig. 7. The same mask as in Fig. 6, after implantation with  $5 \times 10^{16}$  ions/cm<sup>2</sup> Fe<sup>+</sup> at 80 keV. Compared to Fig. 6, the hole bottoms are cleaner.

process had little obvious impact on the mask. In fact, mask sputtering tends to clean the bottoms of holes in the mask that were incompletely etched before implantation. The overall structure of the mask, however, remains intact. This ion-cleaning effect is illustrated in Figure 7, where there is relatively little residual material in the mask holes.

Optical microscopy of the Fe implanted samples was done after chemical removal of the mask (Fig. 7). The features transferred quite well and are readily apparent under standard viewing conditions. Current experiments using oil immersion optical microscopy show that even the 0.5-micron structures are well preserved in the implanted SiO<sub>2</sub> wafer. We are currently investigating the optimal thermal processing parameters to produce "digital block arrays" of Fe nanocrystals. Magnetic and magneto-optic investigations of the patterned specimens are ongoing.

These initial results show that the combination of ion implantation and lithographic masking has promise for extending experimental control into the sub-micron spatial domain. Patterning at smaller scales, however, will present special challenges. Other forms of lithography will be needed to create features smaller than 0.5 microns in diameter, and anisotropic etching techniques will have to be employed to improve the aspect ratio of the mask hole walls. Also, the mask thickness will have to be reduced. Ion-beam scattering effects (both within the mask and within the host material) may become a technical problem at the smallest feature sizes. Nevertheless, these initial results are encouraging, and if the associated materials-related challenges can be met, it may be possible to create patterned arrays of single embedded nanoparticles with controlled size and shape.

## CONCLUSIONS

Two main goals of our work on ferromagnetic nanocluster composites are to obtain fine-scale control over the magnetic properties, and to achieve sub-micron spatial control over the location of these properties. Progress toward achieving these goals has been made in the work presented here, although considerable materials-characterization and theoretical work on the magnetic properties remains to be done. Extensive future and

ongoing work will be required to fine-tune both the spatial and magnetic control aspects of the research in order to obtain implantation-produced nanocomposites that can meet the requirements of specific device-related applications.

## ACKNOWLEDGEMENTS

The authors wish to thank D. Mullen and G. Braybrook for technical support. This research was supported by NSERC. Oak Ridge National Laboratory is managed by UT-Battelle, LLC, for the U.S. Department of Energy under Contract No. DE-AC05-00OR22725

## REFERENCES

1. C. W. White, C. J. McHargue, P. S. Sklad, L. A. Boatner, and G. C. Farlow, *Materials Science Reports* **4**, 41-146 (1989). For a recent review see: A. Meldrum, R.F. Haglund, L.A. Boatner, and C.W. White, *Adv. Mater.* **13**, 1431 (2001).
2. D.N. Lambeth, E.M.T. Velu, G.H. Bellesis, L.L. Lee, and D.E. Laughlin, *J. Appl. Phys.* **79** (1996) 4496.
3. S. Honda, F. A. Modine, T.E. Haynes, A. Meldrum, J.D. Budai, K. J. Song, J.R. Thompson, and L.A. Boatner, *Mat. Res. Symp. Proc.* **581**, 71-76 (2000).
4. S. Honda, F.A. Modine, A. Meldrum, J.D. Budai, T.E. Haynes, L.A. Boatner, and L.A. Gea, *Mat. Res. Symp. Proc.* **540**, 225-230 (1999).
5. T.C. Schulthess, M. Benakli, P.B. Visscher, K.D. Sorge, J.R. Thompson, F.A. Modine, T.E. Haynes, L.A. Boatner, G.M. Stocks, W.H. Butler, *J. Appl. Phys.* **89**, 7594 (2001).
6. A. Meldrum, K.S. Beaty, M. Lam, C.W. White, R.A. Zuhr, and L.A. Boatner (these proceedings).
7. N.M. Dempsey, X.L. Rao, J.M.D. Coey, J.P. Nozieres, M. Ghidini, B. Gervais, *J. Appl. Phys.* **83**, 6902 (1998).
8. W. J. Weber, *Nucl. Instr. Meth.* **166**, 98 (2000).
9. J. W. Mayer, L. Eriksson, and J. A. Davies, *Ion Implantation in Semiconductors* Academic Press, New York (1970).
10. C. Chappert, H. Bernas, J. Ferre, V. Kottler, J.-P. Jamet, Y. Chen, E. Cambril, T. Devolder, F. Rousseaux, V. Mathet, H. Lanois, *Science* **280**, 1919 (1998).
11. S. Honda, F. A. Modine, A. Meldrum, J.D. Budai, T. E. Hayes, and L. A. Boatner, *Appl. Phys. Lett.* **77**, 711 (2000).
12. E. Alves, C. MacHargue, R. C. Silva, C. Jesus, O. Conde, M.F. da Silva, and J. C. Soares, *Surf. Coat. Tech.* **128-129**, 434 (2000).

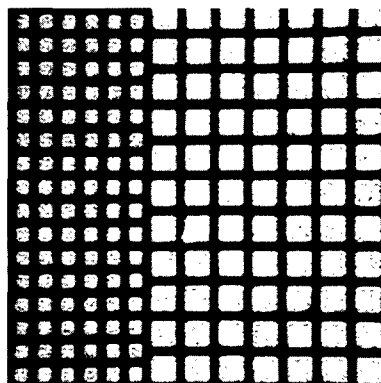


Fig. 8. Optical image of a specimen implanted with  $1.5 \times 10^{17}$  ions/cm<sup>2</sup> of Fe. The mask has been removed and the bright regions correspond to the implanted area. The edge length of the large squares is 12 um.